Analysis of nonideal Schottky and *p-n* junction diodes—Extraction of parameters from *I–V* plots

M. Lyakas,[a] R. Zaharia, and M. Eizenberg
Department of Materials Engineering and Solid State Institute, Technion–Israel Institute of Technology, Haifa 32000, Israel

(Received 5 May 1995; accepted for publication 11 July 1995)

We propose two novel methods of determining nonideal Schottky and *p-n* junction diodes parameters from *I–V* plots. The series resistance R_s, saturation current I_s, as well as the bias-dependent ideality factor $n(V)$, can be obtained from two successive *I–V* measurements—one solely of the diode and the other with an external resistance added in series with the measured diode. Our analysis confirms that the methods produce accurate and reliable results even when the conventional techniques fail, such as when we have strongly varying function $n(V)$ in the presence of series resistance and an experimental noise. © *1995 American Institute of Physics.*

I. INTRODUCTION

I–V measurements are widely used to characterize the barrier height, carrier transport mechanisms, and interface states in Schottky barriers and *p-n* junctions.[1–3] The extraction of the diode parameters is usually complicated by their voltage dependence and the presence of series resistance. Therefore, the interpretation of the experimental *I–V* data must be performed with care. This is widely discussed by many authors.

Usually, the parameters that describe a current flow across a Schottky or a *p-n* junction diode are introduced in such a way that the experimental *I–V* plot can be represented by the equation

$$I=I_s\left[\exp\left(\frac{q(V-IR_s)}{nkT}\right)-1\right], \tag{1}$$

where I is the diode current, I_s the saturation current, q the electron charge, V the applied bias voltage, R_s the series resistance, n the ideality factor, k the Boltzman constant, and T the temperature.

The saturation current I_s depends on the carrier transport mechanism across the structure. For thermionic emission in Schottky barriers,

$$I_s=AA^{**}T^2\exp\left(-\frac{q\phi_{b0}}{kT}\right). \tag{2}$$

Here A is the contact area, A^{**} the effective Richardson constant, and ϕ_{b0} is the zero voltage barrier height.

A simplified expression is widely used to describe the current flow only under forward bias when $(V-IR_s)\geq 3kT/q$,

$$I=I_s\exp\left(\frac{q(V-IR_s)}{nkT}\right). \tag{3}$$

The representation of the diode current via Eqs. (1) and (3) means that the formally introduced ideality factor should reflect all the deviations of the current flow from the ideal model, including such known effects as: image force and field-induced Schottky barrier lowering, presence of interface states, generation–recombination current, tunneling across the interface, high level of injection, and spatial barrier inhomogeneities. Hence, it is difficult to expect, *a priori*, that the ideality factor of a real diode will have a constant value; it should rather be a function of the applied voltage.

Based on this we consider briefly the main features of the conventional methods to extract the parameters from *I–V* plots. In the following sections we propose a new approach to analyze the parameters of a real diode from *I–V* plots both for a voltage-independent and for a voltage-dependent ideality factor. This is illustrated by a specific example of Schottky diodes. In the discussion below we assume that all the deviations of the ideality factor from unity and its voltage dependence only result from the voltage dependence of the Schottky barrier height, so that the current transport through the structure can be described by Eqs. (1)–(3).

II. CONVENTIONAL METHODS FOR ANALYSIS OF *I–V* PLOTS

The most widely used methods to extract the diode parameters can be divided into several main groups:

(1) analysis of the linear part of $\ln I$ vs V plot;[1–3]
(2) construction of Norde[4] or Norde-like[5–7] plots;
(3) utilization of the small signal conductance $G=dI/dV$.[8,9]

In addition, one can find various methods based on the integration of the current with respect to the bias voltage[10] and on the fitting of the parameters.[7,11–14] Recently Evangelou *et al.*[14] demonstrated a fitting procedure which produces more accurate results than other methods in the presence of experimental noise. However, the main limitation of the fitting methods was highlighted by Werner,[9] who pointed out that the numerical coincidence between the measured and fitted data only is not sufficient to prove the validity of the diode model. In addition, the multidimensional fitting procedures are time consuming.

The main advantages and limitations of the known techniques are analyzed in many reports.[1–3,9,14,15] It was pointed out that, in spite of some pitfalls, Werner's plot A[9] seems to be the most sensitive and reliable for obtaining the voltage-

[a]Electronic mail: mtrlia@vmsa.technion.ac.il

 0021-8979/95/78(9)/5481/9/$6.00

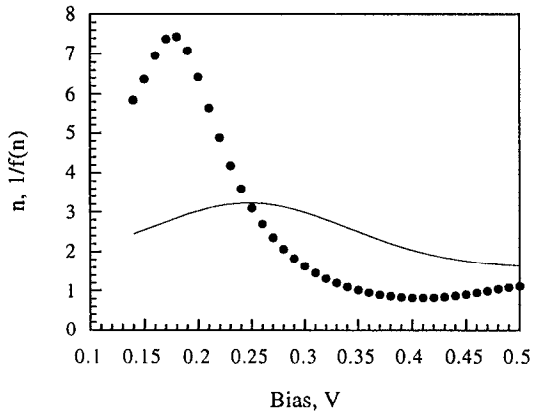

FIG. 1. Voltage-dependent ideality factor observed for Au/n-GaAs Schottky diodes (Ref. 16) (solid curve) and the function $f(n)^{-1}=\{(kT/q)[d(\ln I)/dV\}^{-1}$, obtained by numerical differentiation of a theoretically simulated $I-V$ plot (dotted curve).

independent real Schottky and p-n junction diode parameters.[15] However, the common approach is that all the diode parameters introduced into Eqs. (1)–(3) are assumed to be voltage independent.

Only a few methods, to the best of our knowledge, have been proposed to analyze Schottky and p-n junction diodes with a voltage-dependent ideality factor $n(V)$. One of the most widely accepted procedures (see, for example, Refs. 1 and 3) utilizes the differentiation of the simplified expression (3), so that the ideality factor is calculated as

$$\frac{1}{n(V)}=\frac{kT}{q}\frac{\partial}{\partial V}(\ln I). \tag{4}$$

However, numerical differentiation in accordance with Eq. (4) is, in effect, a complete and not a partial differentiation, as required. The resulting function is, in fact, not the true ideality factor $n(V)$ but rather some function $f(n)$ of it,

$$f(n)=\frac{kT}{q}\frac{d}{dV}(\ln I)=\frac{1}{n}-\frac{V}{n^2}\frac{dn}{dV}. \tag{5}$$

If the value of $dn(V)/dV$ is not significantly lower than the value of $n(V)/V$ at the same bias, then the second term in the right-hand side of the above equation cannot be neglected. Therefore, the exact values of the ideality factor should be obtained by integration of the differential equation (5). Generally, this procedure is complicated due to unknown initial condition; only for the points where $dn(V)/dV=0$ does the ideality factor $n(V)$ equal $1/f(n)$. This is illustrated in Fig. 1 where an ideality factor with a strong deviation due to the presence of interface states, observed in Au/n-GaAs Schottky diodes,[16] was used to simulate a theoretical $I-V$ plot without a series resistance. Then the numerical differentiation of this plot was performed to extract the ideality factor according to Eq. (4). One should agree that the calculation results essentially differ from the input hypothetical ideality $n(V)$.

The way[17] to calculate the function $n(V)$ at each point of the experimental $I-V$ data using the equation

$$n(V)=\frac{qV}{kT}\ln^{-1}\left(\frac{I}{I_s}+1\right) \tag{6}$$

assumes that the saturation current I_s is previously determined. Another method to obtain the bias-dependent Schottky barrier height by comparing the real $I-V$ plot with the hypothetical ideal one is considered in Refs. 16 and 17. All the methods proposed by the above group produce correct results only assuming that the influence of the series resistance is negligible.

It follows that new considerations must be taken into account when real diodes showing nonlinearity in their semilogarithmic plots are treated in order to extract their parameters.

III. NOVEL METHODS PROPOSED FOR THE DETERMINATION OF REAL DIODE PARAMETERS

The methods proposed below are based on the effect of the series resistance on the diode $I-V$ characteristics. The essence of the proposed methods is to carry out two consecutive measurements:

(i) conventional $I-V$ measurement of the diode and
(ii) $I-V$ measurement after adding an external resistance R_{ex} in series with the diode.

By applying Eq. (3) to each of the above-mentioned measurements, we obtain the following set of equations:

$$\ln I-\ln I_s=\frac{q(V-IR_s)}{n(V)kT},$$
$$\frac{\Delta(\ln I)}{R_{ex}}=-\frac{q}{n(V)kT}\left((R_s+R_{ex})\frac{\Delta I}{R_{ex}}+I\right), \tag{7}$$

where $\Delta(\ln I)$ and ΔI are the corresponding changes in $\ln I$ and I at a given bias voltage V produced by adding the additional resistance R_{ex} in series with the diode. Note that ΔI and $\Delta(\ln I)$ are always negative.

The set of Eqs. (7) allows one to establish relationships between any two of the three unknown diode parameters. This provide the basis to develop two novel methods for data treatment. The first method (method A) utilizes a relationship between the ideality factor and the saturation current,

$$f_2(I,\Delta I)=\ln I_s+\frac{q}{n(V)kT}f_1(V,I,\Delta I,R_{ex}), \tag{8}$$

where

$$f_1(V,I,\Delta I,R_{ex})=V+IR_{ex}\left(1+\frac{I}{\Delta I}\right) \tag{9}$$

and

$$f_2(I,\Delta I)=\ln I-\frac{I}{\Delta I}\ln\left(1+\frac{\Delta I}{I}\right). \tag{10}$$

Functions f_1 and f_2 contain only experimentally measurable quantities, therefore Eq. (8) represents the modified form of the expression (3), where the unknown value of R_s is avoided. By these means both the saturation current I_s and the ideality factor $n(V)$ can be obtained from the slope and

the vertical axis intercept of the f_2 vs f_2 plot independently of the series resistance. Then the series resistance R_s can be calculated, for instance, from Eq. (3) or from the following Eq. (11).

The second method (method B) follows from another relationship between the saturation current and the series resistance which can also be derived from the set of Eqs. (7),

$$R_s = -\frac{1}{\Delta I}\left[\frac{f_1}{f_2 - \ln I_s}\ln\left(1+\frac{\Delta I}{I}\right) + R_{ex}(I+\Delta I)\right]. \quad (11)$$

Assuming, as usual, both the saturation current and the series resistance to be bias independent over the range of interest, Eq. (11) offers two possibilities to obtain these parameters. The first originates from the condition $dR_s/dV=0$; the differentiation of the right-hand side of Eq. (11) leads to a quadratic equation with two analytically derived roots,

$$(\ln I_s)_{1,2} = f_2 - \left\{\frac{f_3'}{2f_2'f_3}\left[1 \pm \left(1+\frac{4R_{ex}f_3f_2'f_4'}{(f_3')^2}\right)^{1/2}\right]\right\}^{-1}. \quad (12)$$

Here $f_3 = f_1 \ln[1+(\Delta I/I)]/\Delta I$, $f_4 = 1+(I/\Delta I)$, and the prime represents the derivative with respect to the bias voltage. Similarly to Eq. (8) all the functions in Eq. (12) contain only measurable amounts. The analysis of the behavior of the roots shows that one of them, namely the one with the sign "+", is bias independent and corresponds to a physically meaningful value of I_s, while the second root changes with the bias to ensure the constant value of R_s.

Another approach is based on the observation that the difference of the two strongly bias depending terms in Eq (11) should produce the bias-independent value of R_s. The only unknown parameter here to satisfy this condition is $\ln I_s$, which can be obtained by fitting. The fitting criterion may be, for example, the minimum of the standard deviation of the calculated values of R_s over the analyzed bias range. The obtained values of $\ln I_s$ and R_s can then be used to extract the voltage-dependent ideality $n(V)$ according to Eq. (3).

The selection of an optimal value for R_{ex} is dictated by two opposing considerations. On the one hand, the value of the additional resistor should be large enough to obtain a meaningful current change at a given bias voltage. On the other hand, the addition of R_{ex} produces an additional shift ΔV_R in the diode voltage V_d [since $V_d = V - I(R_s + R_{ex})$], which leads to a possible error in the determination of $n(V)$. It should be noted, that the second equation in Eq. (7) was derived neglecting this effect. Therefore, the upper limit of R_{ex} should be determined by the requirement that the change $\Delta n = (dn/dV_d)\Delta V_R$ produced by the voltage shift ΔV_R must be much smaller than the value of $n(V)$ at the same diode voltage. It can be easily shown that it leads to the following evaluation:

$$\frac{R_{exmax}}{R_s} = \left(\frac{\alpha}{IR_s}\frac{n(V_d)}{|n'(V_d)|}+1\right)\exp\left(\frac{q\alpha}{|n'(V_d)|kT}\right) - 1, \quad (13)$$

where R_{exmax} is the maximal allowed value of R_{ex}, α is the required relative accuracy of the determination of n, and $n'(V_d) = dn(V_d/dV_d)$.

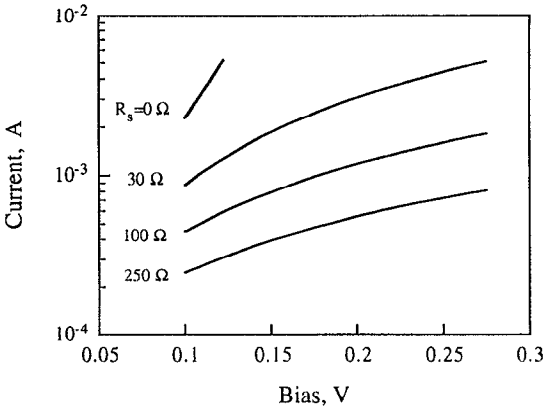

FIG. 2. $I-V$ plots calculated for Schottky diodes with bias-independent parameters: $\phi_{b0}=0.45$ eV, $n=1.08$, $A^{**}=32$ A cm^{-2} K^{-2}, and different values of series resistance: $R_S=0$, 30, 100, and 250 Ω.

The lower limit of R_{ex} can be defined by the minimal requirement that $|\Delta I/I| > \delta I$, where δI is the relative experimental noise of the measured diode current. Using the second of Eqs. (7) we obtain for $\Delta I \ll I$ and $\delta I \ll 1$

$$\frac{R_{ex\ min}}{R_s} > \delta I\left(\frac{n(V)kT}{qIR_s}+1\right). \quad (14)$$

Equations (13)–(14) along with the above-mentioned measurable quantities contain all the required information about the diode parameters. To perform the parameter extraction, the initial values of R_s and $n(V)$ can be estimated either by measuring at any small magnitude of R_{ex} followed by repeated measurements with it increasing values or by using other evaluation methods. Then the values of R_s and $n(V)$ may be precisely obtained by evaluating the upper and lower limits of R_{ex} from Eqs. (13)–(14) and carrying out the measurements according to the described procedures.

IV. VERIFICATION OF METHODS

The validity of the proposed methods was examined by analyzing theoretically calculated $I-V$ characteristics of Schottky diodes with different series resistances $R_s=0$, 30, 100, and 250 Ω. For all the simulations contact area was 0.16 mm^2 and the temperature 20 °C. After addition of random electronic noise the simulated $I-V$ data were smoothed for the following evaluation.

A. Voltage-independent parameters

The proposed methods A and B were applied to examine the theoretically calculated $I-V$ plots typical for W/p-Si Schottky diodes with low barrier height when n differs from unity ($\phi_{b0}=0.45$ eV,[3] $n=1.08$). The effective Richardson constant was taken to be $A^{**}=32$ A cm^{-2} K^{-2}. These plots, as is presented in Fig. 2, have no linear parts suitable for conventional analysis. Regarding the bias-independent ideality the value of R_{ex} is not limited from above and can be chosen arbitrarily. Figure 3 (solid curve) shows that the corresponding f_2 vs f_1 plot (method A), calculated for $R_s=100$ Ω and $R_{ex}/R_s=0.2$ from Eqs. (9) and (10), represents the straight line. The f_2 vs f_1 plots calculated for different R_s and R_{ex},

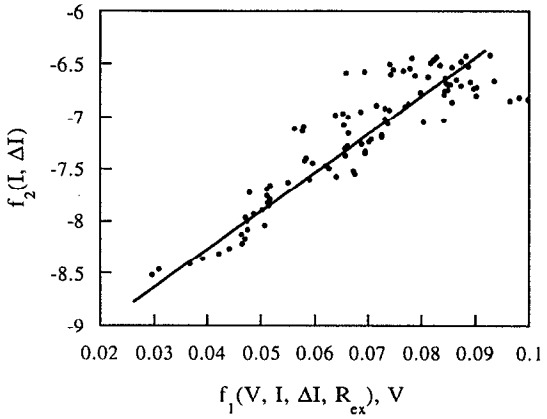

FIG. 3. f_2 vs f_1 plot of method A calculated for corresponding $I-V$ plot (Fig. 2) with $R_S=100\ \Omega$ and $R_{ex}/R_S=0.2$ in the absence of noise (solid curve) and for a 0.5% random noise (dots).

with the other parameters unchanged, only slide over one another with the same slope and f_2 axis intercept. The results of the parameter extraction for various R_s and R_{ex} in the absence of electronic noise showed that the accuracy of the proposed methods depends only on the accuracy of the simulations.

When the scattering of the $I-V$ data is taken into account, the accuracy generally tends to decrease. This is illustrated in Fig. 3 which also gives an example of an f_2 vs f_1 plot calculated from the same $I-V$ plot (for $R_s=100\ \Omega$ and $R_{ex}/R_s=0.2$) in the presence of 0.5% random electronic noise. The corresponding bias dependencies of R_{exmin}/R_s calculated from the $I-V$ plots according to Eq. (14) are shown in Fig. 4; the maximal ratio of R_{exmin}/R_s for $R_s=100\ \Omega$ is less than the selected value of R_{ex}/R_s by a factor of approximately 25. The influence of the noise on the f_2 vs f_1 plot tends to increase with a rise of the diode current; this effect is discussed below. Since the low-bias region is usually not reliable for the analysis due to leakage currents, Eqs. (8) and (11) were utilized to extract the constant Schottky diodes parameters over the intermediate region of the current, containing approximately 2/3 of all calculated points. Equation (11) was solved analytically [Eq. (12)] as well as by fitting of $\ln I_s$.

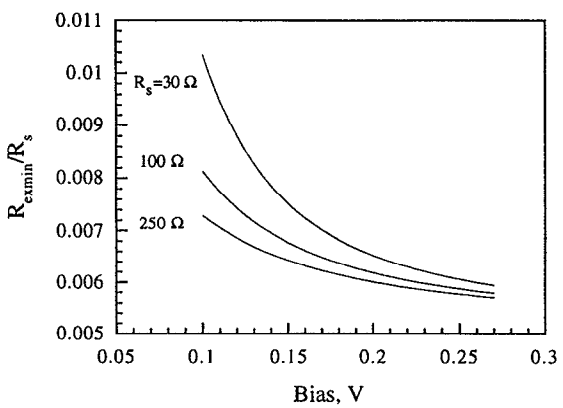

FIG. 4. Function $R_{ex\ min}/R_S$ calculated from the corresponding $I-V$ plots (Fig. 2) with various series resistance ($R_S=30$, 100, and 250 Ω) for 0.5% random noise.

Our analysis was compared to that of Werner's method.[9] The above-mentioned $I-V$ plots ($R_s=30$, 100, and 250 Ω) after addition of 0.5% random electronic noise were smoothed and Werner's plot A was applied to extract the diode parameters. Upon the corresponding correction of the voltage axis the analysis yielded the following set of parameters: $n=1.24$, $\phi_b=0.4421$ eV, $R_s=27.4\ \Omega$; $n=1.58$, $\phi_b=0.437$ eV, $R_s=81.6\ \Omega$; and $n=1.85$, $\phi_b=0.435$ eV, $R_s=197.8\ \Omega$, respectively. Such deviations between the de-

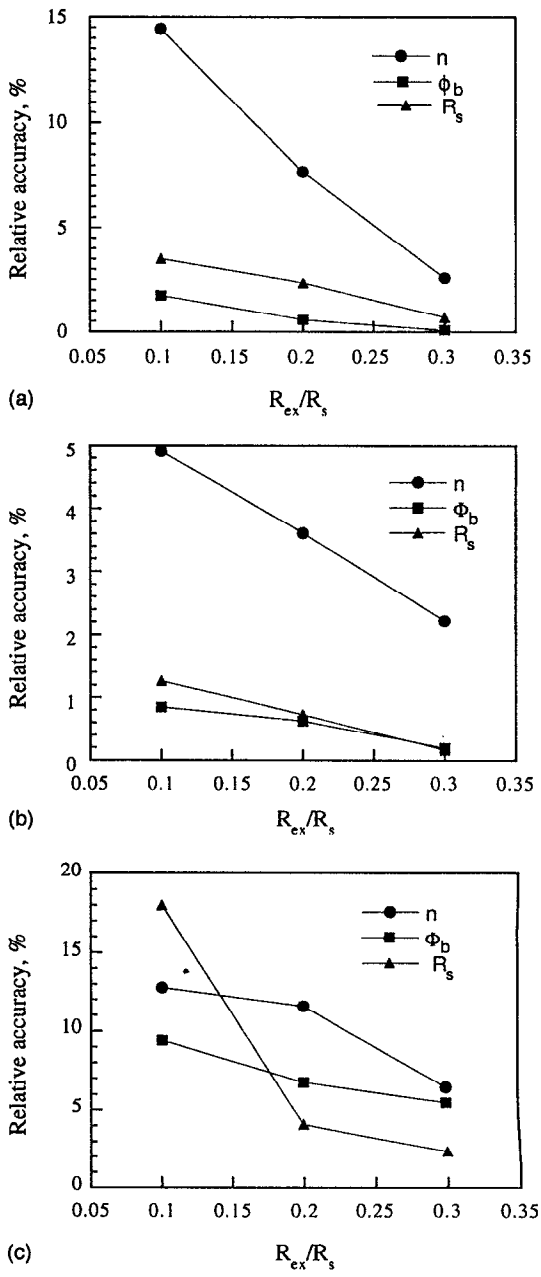

FIG. 5. Relative accuracies for the extraction of bias-independent Schottky diode parameters from $I-V$ plot of Fig. 2 ($R_S=100\ \Omega$) for 0.5% electronic noise: (a) method A; (b) method B—fitting; (c) method B—analytical solution.

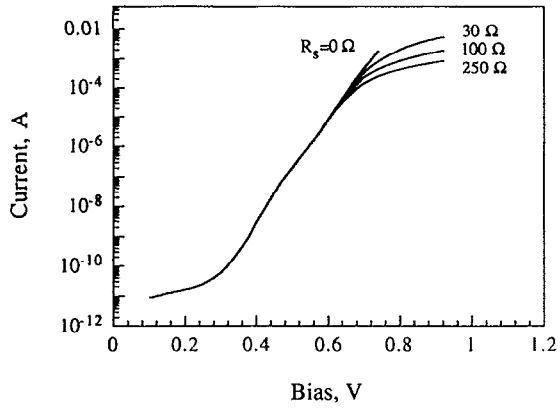

FIG. 6. $I-V$ plots calculated utilizing the voltage-dependent ideality factor, presented in Fig. 1, for different values of series resistance: R_S=0, 30, 100, and 250 Ω. The other parameters are: A^{**}=4.4 A cm^{-2} K^{-2}, ϕ_{b0}=0.88 eV.

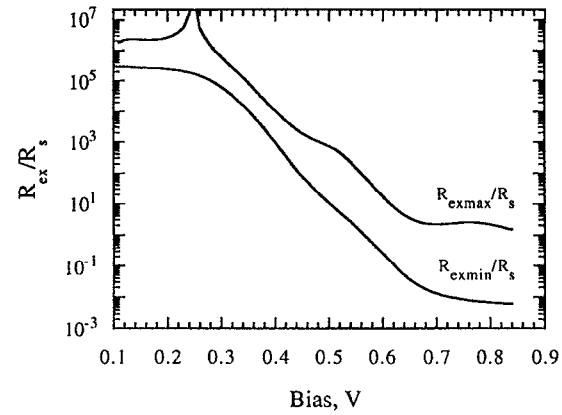

FIG. 7. Calculated maximal and minimal allowed values of R_{ex}/R_S for $I-V$ plot (see Fig. 6) with R_S=100 Ω in the presence of 0.5% randomly distributed electronic noise.

termined and the nominal values of the parameters evidence the increasing sensitivity of Werner's method to experimental noise with the increase of R_s, especially for low barrier heights. This was also pointed out in Refs. 14 and 15.

Typical relative accuracies for the extracted values of the bias-independent parameters obtained by the proposed methods are presented in Figs. 5(a), 5(b), and 5(c). The analysis was performed in the presence of a randomly distributed 0.5% electronic noise for R_s=100 Ω. As one would expect, the accuracy of the proposed methods increases rapidly with the increase of R_{ex}/R_s. The fitting algorithm of method B turns out to produce the most accurate results. The series resistance R_s obtained with high accuracy from all the procedures can be used to calculate the corrected ln $I-V_d$ plots and to extract the ideality factor and the saturation current I_s more accurately.

B. Voltage-dependent parameters

The advantages of the proposed methods are seen most clearly when diodes with voltage-dependent parameters are treated. We used a strongly varying ideality factor $n(V)$, as given in Ref. 16 (Fig. 1), to simulate $I-V$ plots of Au/n-GaAs Schottky diodes with R_s=0, 30, 100, and 250 Ω. The other parameters of the diodes were A^{**}=4.4 A cm^{-2} K^{-2} and ϕ_{b0}=0.88 eV.[1] The calculated plots are presented in Fig. 6. Obviously, the known techniques are not applicable to the analysis of such nonlinear semilogarithmic $I-V$ plots.

The function R_{exmax}/R_s was then calculated assuming that the allowable error in the determination of $n(V)$ should not exceed 1%. The result for R_s=100 Ω is presented in Fig. 7. The features of the R_{exmax}/R_s plot are mainly determined by the behavior of the derivative dn/dV_d; in particular, the sharp peak at ≈0.25 V is attributed to the global maximum of function $n(V_d)$, where dn/dV_d=0. For our specific case of a very strongly varying function $n(V)$ and R_s=100 Ω the value $R_{exmax}/R_s \approx 1$ ensures the determination of $n(V)$ in the whole voltage range with an accuracy not worse than 1%.

The typical transformed carrier transport equation (8) recalculated for R_s=100 Ω and R_{ex}/R_s=1 demonstrates the strong nonlinearity in the whole voltage range as is presented in Fig. 8 (solid curve). Following the approach of Ref. 3 one can assume that a possible voltage dependence of the effective Richardson constant A^{**} may also be included in the voltage dependence of the ideality factor. In this manner all the deviations of the f_2 vs f_1 plot from linearity should be ascribed to the bias dependence of $n(V)$ alone. Nevertheless, our method A does not provide the possibility of extracting the parameters from nonlinear ln $I-V$ plots in general, due to the reasons previously discussed in Sec. II. The numerical differentiation of the function f_2 with respect to f_1 yields the new function $\varphi(n)$,

$$\varphi(n)=\frac{kT}{q}\frac{df_2}{df_1}=\frac{1}{n}-\frac{f_1}{n^2}\frac{dn}{df_1}. \tag{15}$$

The exact solution of Eq. (15) can be obtained only in the special case that after the integration with an arbitrary initial condition one finds some extrema of the calculated function $n(V)$. These points can then be considered as initial conditions for further exact integration.

The application of method B generally allows us to derive all the parameters, even for this strongly nonlinear occasion. As in the case of the constant Schottky diode param-

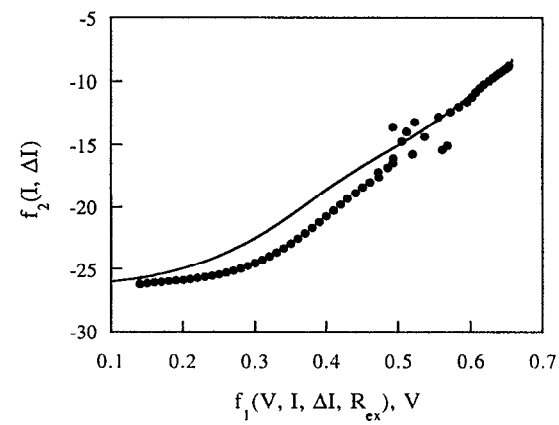

FIG. 8. f_2 vs f_1 plot of method A calculated from the corresponding I–V plot (Fig. 6) with R_S=100 Ω and R_{ex}/R_S=1 in the absence of noise (solid curve) and for 0.5% random noise (dots).

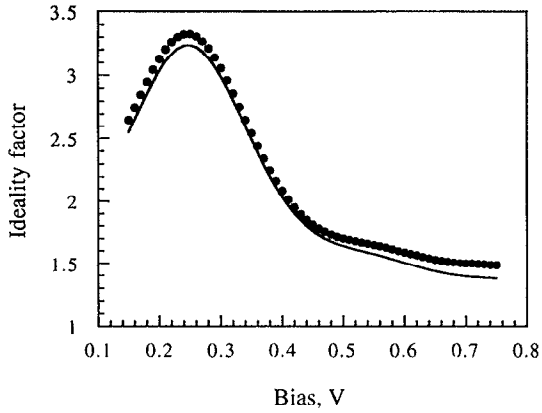

FIG. 9. Hypothetical (solid curve) ideality and ideality (dotted curve) extracted by fitting of Eq. (11) from $I-V$ plot (Fig. 6). The parameters used are: $R_S=100\ \Omega$; $R_{ex}/R_S=1$; noise=0.5%.

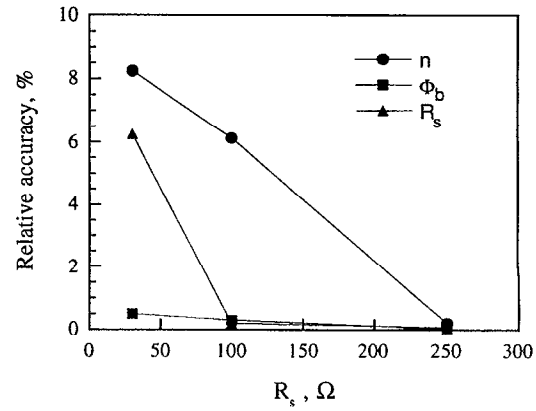

FIG. 10. Statistically evaluated accuracies for the extraction of diode parameters from $I-V$ plot of Fig. 6 ($R_{ex}/R_s=1$, noise=0.5%) by fitting of Eq. (11).

eters, utilization of this method to study the plots presented in Fig. 6 revealed that the accuracy of the parameter extraction in the absence of electronic noise depends only on the accuracy of the simulations. The addition of electronic noise to the calculated plots also gives rise to errors in the determination of parameters. Figure 8 (dots) shows the above f_2 vs f_1 plot in the presence of 0.5% random electronic noise. As opposed to the case of low barrier height (see Fig. 3) the scattering is considerably reduced almost for all data points. The corresponding plot of R_{exmin}/R_s calculated for 0.5% random noise is also presented in Fig. 7. One can see that for this particular case of a strongly deviating ideality factor it is impossible to determine the diode parameters accurately by using a single value of R_{ex} for the whole voltage range. The selected value $R_{ex}/R_s=1$ makes an accurate determination of the parameters possible only for bias voltages above $\approx$0.6 V. This corresponds to the values of the function f_1 beyond $\approx$0.52 V. The f_2 vs f_1 plot below this point is shifted with respect to the true curve, as is seen in Fig. 8; this stems from the influence of noise on the current difference ΔI. This effect is discussed below. Taking into account that the low-current region is dominated by leakage currents and that the instrumental accuracy of the measurements is better for the larger currents, we have selected the value of $R_{ex}/R_s=1$, which ensures the correct analysis of the intermediate- and high-current regions (above $\approx$0.6 V). The extracted values of I_s and R_s were then substituted into Eq. (3) to obtain the ideality factor in the whole voltage range. A typical result of the $n(V)$ extraction by fitting of Eq. (11) is shown in Fig. 9. The extracted $n(V)$ is very close to the actual $n(V)$ function.

The statistical evaluation of the maximal errors in the parameters, which were obtained by fitting of Eq. (11), as a function of the diode series resistance R_s are presented in Fig. 10. The evaluation was carried out for 0.5% random noise using $R_{ex}/R_s=1$. As evident from these data the accuracy have a general trend to increase with the increase of the series resistance R_s, in contrast to the method of Ref. 9. As for the results of Sec. IV A, the extraction accuracy rapidly increases with the increases of the ratio R_{ex}/R_s up to its maximum allowed value.

V. IMPLEMENTATION OF THE METHOD FOR EXPERIMENTAL DIODES

The new method enabled us to analyze actual experimental $I-V$ plots of Pd–$Si_{0.9}Ge_{0.1}$/Si Schottky diodes prepared by vacuum annealing at 250 °C for 30 min. $I-V$ plots measured at room temperature with voltage step of 10 mV and various R_{ex} (0, 3.9, and 39.2 Ω) are shown in Fig. 11. The corresponding Werner's[9] plot A calculated for $R_{ex}=0$ (see Fig. 12) reveals a weak nonlinearity over a few decades of the diode current. Therefore, the linear fit yields the parameters averaged over the selected range. The parameters obtained by this method were: $n=1.05$; $R_s=13.8\ \Omega$; and $I_s=1.45\times10^{-7}$ A.

The fitting algorithm of our method B applied to the analysis of the $I-V$ plots (Fig. 11) yielded the values $R_s=12.3\ \Omega$, $I_s=1.45\times10^{-7}$ A for $R_{ex}=3.9\ \Omega$ and $R_s=12.6\ \Omega$, $I_s=1.46\times10^{-7}$ A for $R_{ex}=39.2\ \Omega$. The ideality factor obtained slightly changes from 1.04 to $\approx$1.1 in the range covered (see Fig. 13). The validity of the values used for R_{ex} was verified by the calculation of its maximum and minimum allowed values, as is shown in Fig. 14. We note that the magnitude of $R_{ex}=3.9\ \Omega$ as well as $R_{ex}=39.2\ \Omega$ can be

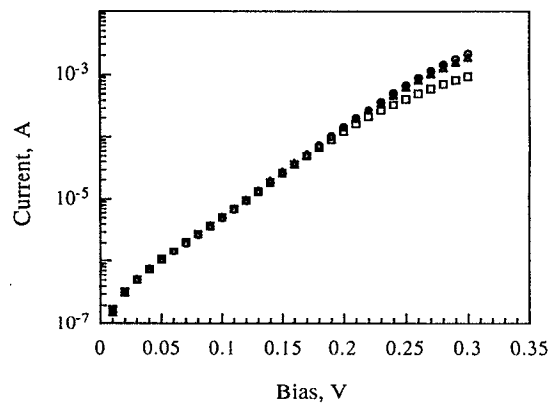

FIG. 11. $I-V$ plots of Pd–$Si_{0.9}Ge_{0.1}$/Si Schottky diode measured with various external resistances: $R_{ex}=0$ (circles), 3.9 (triangles), and 39.2 (squares) Ω.

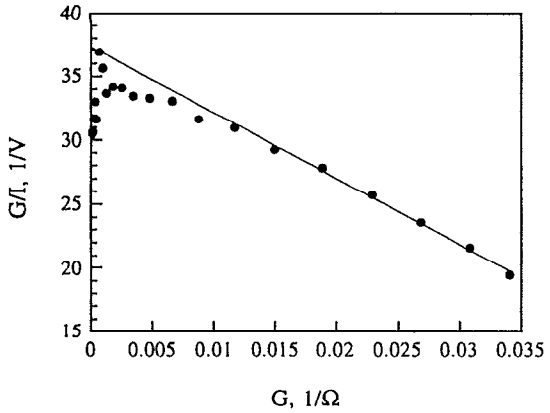

FIG. 12. Werner's (Ref. 9) plot A of Pd–$Si_{0.9}Ge_{0.1}$/Si Schottky diode measured without an external resistance. Experimental points (dots) and linear fit (solid line).

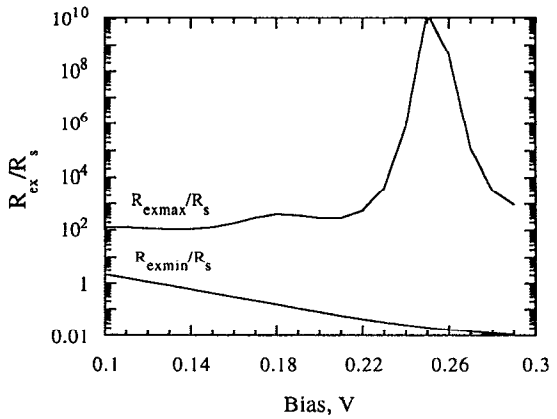

FIG. 14. Maximal and minimal ratios of R_{ex}/R_S for $I-V$ plots from Fig. 11 in the presence of 0.5% experimental noise. Predetermined accuracy of extraction of the ideality factor is better than 1%.

utilized for the diode analysis in the measured voltage range. As a consequence, both the constant diode parameters R_s and I_s and the functions $n(V)$, obtained by using $R_{ex}=3.9$ and 39.2 Ω, are very close. The departures from values of the parameters obtained by Werner's method are obviously attributed to the slight increase of $n(V)$ in the region of evaluation, which results in an increase of the vertical axis intercept and in a decrease of the horizontal axis intercept of G/I vs G plot. Therefore, when using Werner's plot, the value of R_s should be larger and the averaged value of n smaller than the true values.

VI. DISCUSSION

We have shown that an additional measurement with an external series resistance allows one to transform the ideal carrier transport Eq. (3) so as to reduce the number of unknown parameters to two. The addition of noise mainly results in the scattering of the obtained function $\Delta I(I)$; the effect is proportional to $|I/\Delta I|\,\delta I$. Increasing the diode current gives rise to a monotonous increase of the current difference ΔI. Therefore, the influence of the noise should be more apparent at low currents where the values $I/\Delta I$ and their scattering can be very large.

However, the proposed methods A and B have a distinct sensitivity to the scattering of the data which originates from the different algorithms of the data treatment. Method A utilizes Eq. (8) which represents the modified form of the conventional $\ln I-V$ plot, but avoids the series resistance. Fig-

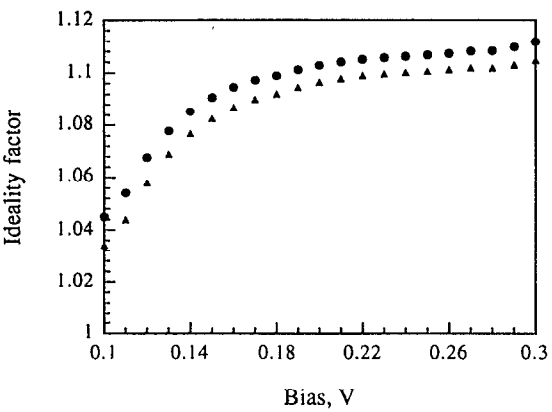

FIG. 13. Voltage-dependent ideality factor of Pd–$Si_{0.9}Ge_{0.1}$/Si Schottky diode extracted by method B (fitting). $R_{ex}=3.9$ Ω (circles) and 39.2 Ω (triangles).

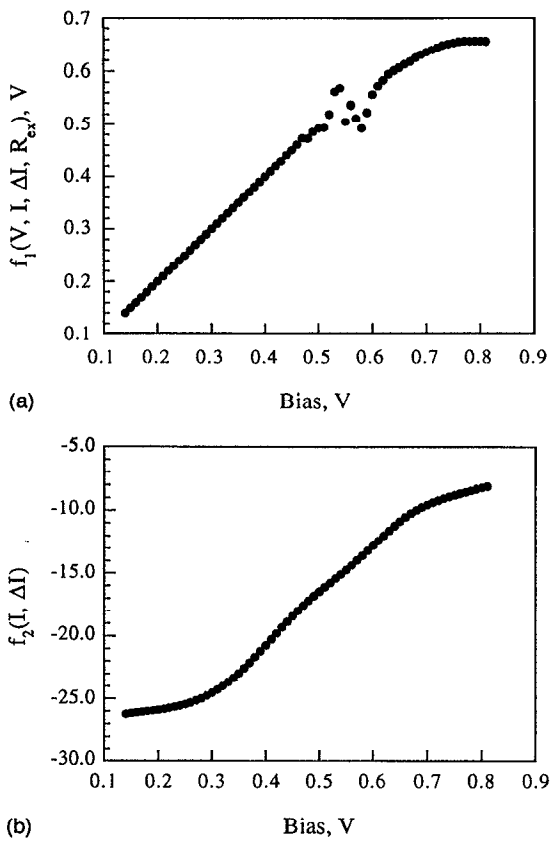

FIG. 15. Typical behavior of the functions (a) f_1 and (b) f_2 recalculated from the $I-V$ plot (Fig. 6) with $R_S=100$ Ω, $R_{ex}/R_S=1$, and 0.5% random noise.

ures 15(a) and 15(b) shows typical behavior of the functions $f_1(V,I,\Delta I,R_{ex})$ and $f_2(I,\Delta I)$, recalculated from the theoretically simulated and smoothed $I-V$ plot of Fig. 6 with $R_s=100\ \Omega$ and $R_{ex}/R_s=1$ in the presence of 0.5% random noise. Depending on the selected value of R_{ex}/R_s [which influences the dependence $\Delta I(I)$] function f_1 compresses the data, especially in the low- and high-current regions, compared to the conventional $\ln I-V$ plot. More rigorously, it shifts the external bias scale V toward the true diode voltage $V_d=V-IR_s$. Function $f_2(I,\Delta I)$ distributes the current data almost uniformly in a logarithmic scale. By this means the f_2 vs f_1 plot emphasizes data and averages extracted values of Schottky diode parameters mostly for intermediate currents.

The effect of noise on the function f_1 depends on the properties of the term $IR_{ex}[1+(I/\Delta I)]$ in the right-hand side of Eq. (9). Assuming $\delta I>|\Delta I|$ (typical for low currents and/or small values of R_{ex}/R_s), the addition of noise distorts the obtained values of ΔI and, correspondingly, $I/\Delta I$ and causes them to oscillate around zero, thus producing a systematic shift of the function f_1 with respect to the true one. The scattering of the f_1 data is scaled down in this situation as long as $IR_{ex}[1+(I/\Delta I)]\ll V$, e.g., at low currents. The increase of the diode current, and/or of the selected ratio of R_{ex}/R_s, results in meaningful magnitudes of the current difference ΔI on the background of the random noise and the function f_1 takes the correct values starting from the certain point. At the same time this can result in an appreciable scattering of the f_1 data. This situation was revealed in Sec. IV B for the diode with large barrier height. The impact of noise on the function f_1 generally shows a rise with an increase of the diode current and is more considerable for the diodes with low barrier height (Fig. 3). Function f_2, on the other hand, practically is not affected by noise due to its logarithmic character.

Compared to Werner's[9] plot A which is very sensitive to the data scattering, especially for low barrier heights and large series resistances, our proposed method A is less sensitive to experimental noise. At the same time, this method generally does not allow analysis of real diodes with voltage-dependent ideality.

Method B, in turn, utilizes the properties of Eq. (11) by finding the only value of $\ln I_s$ which provides a constant function $R_s(V)$ over a certain voltage range. Two approaches have been pointed out here: the utilization of an analytical solution [by Eq. (12)] and a fitting procedure that provides a more constant value of R_s over the analyzed region. The sensitivity of method B to the departures from the true value of $\ln I_s$ is proportional to $(f_2-\ln I_s)^{-2}$. This suggests that, unlike Eq. (8), the method strongly emphasizes the data at lower currents where the values of the function f_2 are very close to $\ln I_s$. This inherent feature of Eq. (11) ensures the exact extraction of the saturation current and the series resistance on the one hand, and makes it more sensitive to data scattering due to the reasons discussed above, on the other. As for method A the impact of noise at high currents is mainly determined by the features of the functions ΔI and f_1. The application of the analytical solution (12) at every point of the data leads to a greater scattering of the extracted values of I_s and R_s while an effective smoothing of the data takes place during the fitting procedure. The method, by its nature, enables one to analyze real Schottky diodes with a voltage-independent, as well as with a voltage-dependent, $n(V)$.

It follows that the intermediate current region is more reliable for the data treatment by the proposed methods. At the same time this region eliminates the effects of leakage currents, and changes of the series resistance due to heating and high level of carriers injection.[9] The accuracy of both of the proposed methods is improved upon the increase of R_s and R_{ex}, all other parameters being equal, because of the corresponding growth of the current difference ΔI above the background of the existing experimental noise.

Generally speaking, the barrier height of a real Schottky diode should be treated *a priori* as a voltage-dependent parameter due to the various imperfections at the interface. On the other hand, one can encounter deviations of the carrier transport mechanisms from pure thermionic emission. In these cases both Werner's[9] and our f_2 vs f_1 plots, based on the utilization of the pure thermionic emission equation (3), should reveal the deviation from linear behavior. This suggests that the analysis of the $I-V$ characteristics of real diodes should begin with the calculation of one of these plots (preferably f_2 vs f_1 in the presence of the noise) and the linearity should be examined. If the plots are not linear one should assume a voltage-dependent barrier height due to interface states and/or the presence of carrier transport mechanisms other than pure thermionic emission. A comparison of the voltage-dependent ideality factor $n(V)$ extracted by our method B with a voltage-dependent barrier height ϕ_b obtained by independent measurements (for instance, internal photoemission) will help to clarify the physical processes controlling the electrical properties of the diodes.

VII. CONCLUSIONS

The presence of series resistance and a voltage-dependent ideality factor causes considerable complications when analyzing $I-V$ plots of Schottky and p-n junction diodes by the known methods. Two new methods, based on two successive measurements using an external resistance added in series with the measured diode, are proposed to determine all the parameters of a real diode. Both methods produce reliable and reproducible results. While method A is effective for the extraction of the constant diode parameters in the presence of noise, method B provides the possibility of analyzing the general case of a voltage-dependent ideality factor even in the presence of a series resistance and experimental noise—when the usual methods fail.

ACKNOWLEDGMENTS

This work was supported by GIF—German–Israeli Foundation for Scientific Research and Development—and by the Fund for the Promotion of Research at the Technion. One of the authors (M.L.) gratefully acknowledges The Center for Absorption in Science, Ministry of Immigrant Absorption, State of Israel for financial support.

[1] E. H. Rhoderick and R. H. Williams, *Metal-Semiconductor Contacts* (Clarendon, Oxford, 1988).
[2] D. K. Shröder, *Semiconductor Material and Device Characterization* (Wiley, New York, 1990).
[3] S. M. Sze, *Physics of Semiconductor Devices* (Wiley, New York, 1981).
[4] H. Norde, J. Appl. Phys. **50**, 5052 (1979).
[5] K. Sato and Y. Yasumura, J. Appl. Phys. **58**, 3655 (1985).
[6] C.-D. Lien, F. C. T. So, and M.-A. Nicolet, IEEE Trans. Electron Devices **ED-31**, 1502 (1984).
[7] D. Gromov and V. Pugachevich, Appl. Phys. A **59**, 331 (1994).
[8] S. K. Cheung and N. W. Cheung, Appl. Phys. Lett. **49**, 85 (1986).
[9] J. H. Werner, Appl. Phys. A **47**, 291 (1988).
[10] A. Ortiz-Conde, F. J. García Sánchez, J. J. Liou, J. Andrian, R. J. Laurence, and P. E. Schmidt, Solid-State Electron. **38**, 265 (1995).
[11] R. J. Bennet, IEEE Trans. Electron Devices **ED-34**, 935 (1987).
[12] D. Donoval, J. de Souza Pires, P. A. Tove, and R. Harman, Solid-State Electron. **32**, 961 (1989).
[13] T. C. Lee, S. Fung, C. D. Beiling, and H. L. Au, J. Appl. Phys. **72**, 4739 (1992).
[14] E. K. Evangelou, L. Papadimitriou, C. A. Dimitriades, and G. E. Giakoumakis, Solid-State Electron. **36**, 1633 (1993).
[15] V. Aubry and F. Meyer, J. Appl. Phys. **76**, 7973 (1994).
[16] K. Maeda, H. Ikoma, K. Sato, and T. Ishida, Appl. Phys. Lett. **62**, 2560 (1993).
[17] T. Ishida and H. Ikoma, J. Appl. Phys. **74**, 3977 (1993).